Low Angle X-ray Diffraction Studies of Chromatin Structure In Vivo and in Isolated Nuclei and Metaphase Chromosomes

JOHN P. LANGMORE and JAMES R. PAULSON

Biophysics Research Division and Division of Biological Sciences, The University of Michigan, Ann Arbor, Michigan 48109; and Medical Research Council Laboratory of Molecular Biology, Cambridge, England CB2 2QH. Dr. Paulson's present address is Department of Chemistry, St. Olaf College, Northfield, Minnesota 55057.

ABSTRACT Diffraction of x-rays from living cells, isolated nuclei, and metaphase chromosomes gives rise to several major low angle reflections characteristic of a highly conserved pattern of nucleosome packing within the chromatin fibers. We answer three questions about the x-ray data: Which reflections are characteristic of chromosomes in vivo? How can these reflections be preserved in vitro? What chromosome structures give rise to the reflections?

Our consistent observation of diffraction peaks at 11.0, 6.0, 3.8, 2.7 and 2.1 nm from a variety of living cells, isolated nuclei, and metaphase chromosomes establishes these periodicities as characteristic of eucaryotic chromosomes in vivo. In addition, a 30–40-nm peak is observed from all somatic cells that have substantial amounts of condensed chromatin, and a weak 18-nm reflection is observed from nucleated erythrocytes. These observations provide a standard for judging the structural integrity of isolated nuclei, chromosomes, and chromatin, and thus resolve long standing controversy about the "true" nature of chromosome diffraction. All of the reflections seen in vivo can be preserved in vitro provided that the proper ionic conditions are maintained.

Our results show clearly that the 30–40-nm maximum is a packing reflection. The packing we observe in vivo is directly correlated to the side-by-side arrangement of 20–30-nm fibers observed in thin sections of fixed and dehydrated cells and isolated chromosomes. This confirms that such packing is present in living cells and is not merely an artifact of electron microscopy. As expected, the packing reflection is shifted to longer spacings when the fibers are spread apart by reducing the concentration of divalent cations in vitro. Because the 18-, 11.0-, 6.0-, 3.8-, 2.7-, and 2.1-nm reflections are not affected by the decondensation caused by removal of divalent cations, these periodicities must reflect the internal structure of the chromatin fibers.

Packaging of DNA in chromosomes can be best understood in terms of three distinct levels of structure. The lowest level of structure is the nucleosome, a repeating subunit consisting of a highly conserved nucleosome core particle with ~146 base pairs (bp) of DNA wrapped around an octamer of the "core histones" ($H3_2$ $H4_2$ $H2A_2$ $H2B_2$), and a variable amount (20–100 bp) of "linker DNA" probably associated with histone H1 (34, 40). The primary structure of chromosomes is a linear arrangement of nucleosomes along the DNA, the so-called "string of beads." Nucleosome cores have been shown by electron microscopy, neutron scattering, and crystallography to be flattened disks 11.0 nm in diameter and 5.7 nm high with two parallel turns of DNA ~2.8 nm apart (21, 32, 58). At the second level, the "string of beads" is further folded to form the basic chromatin fiber (20, 67, 68). At the third level, the chromatin fibers are further folded into loops anchored together at the axis of the chromatid or on the nuclear matrix (5, 11, 16, 29). Here we describe our x-ray diffraction studies of the second level of chromosome structure, the chromatin fiber.

At this level, the most important structural form is probably

THE JOURNAL OF CELL BIOLOGY · VOLUME 96 APRIL 1983 1120-1131

the 20–40-nm thick fibers, which appear to predominate in sections of whole cells and in vitro under "physiological" salt conditions (18, 19, 67). It is reasonable to focus on the study of these thick fibers in hope of gaining insight into the role of chromatin in gene regulation and replication.

How might nucleosomes be arranged within the thick chromosome fibers? Three possibilities have been suggested; first, helical packing of the nucleosomes to form a coil or solenoid (20, 68); second, clustering of the nucleosomes into 20–40-nm globules called "superbeads" (25, 27, 56); and third, a "twisted zig-zag" packing of the nucleosomes (72). Unfortunately, despite extensive study by x-ray and neutron diffraction, electron microscopy, and electric dichroism, there is not yet enough information to determine which of these general models is more correct, and certainly not enough information to construct a detailed model.

Previous diffraction studies have consistently shown broad rings at ~11, 5.5, 3.8, 2.7 and 2.1 nm, indicative of regular packing of nucleosomes in isolated chromatin. The 3.8-, 2.7- and 2.1-nm reflections seem to come from the internal structure of the nucleosome, since they are observed from dilute isolated nucleosomes whereas the 11.0- and 5.5-nm reflections are not (17, 26, 58). The 11.0- and 5.5-nm reflections are expected to arise from higher order packing of the nucleosome into thick fibers (20, 68). However, the 11.0- and 5.5-nm reflections cannot be taken as evidence for the integrity of chromatin fiber structure since they have often been observed under conditions where thick fibers should not exist, such as after removal of histone H1, after shearing in the procedure of Zubay and Doty (75), or in very low ionic strength (2, 3, 8, 10, 15, 20, 37, 44, 48, 57, 71). In all of these cases, the 11.0- and 5.5-nm peaks probably arise merely from the close contact of nucleosomes in concentrated chromatin gels and not from their packing in thick fibers. Such nonspecific packing would explain the concentration dependence of the 11.0-nm peak in gels (e.g., references 3, 8).

The fact that the diffraction patterns of all isolated chromatin, whether "intact" or demonstrably disassembled, are virtually indistinguishable could indicate that all isolated chromatin has a similar, disordered structure. Such disorder could reflect the nature of nucleosome packing in vivo, or merely the disordering influence of the isolation procedures used. While the former possibility has never been carefully explored, the latter possibility has many precedents in the study of chromosomes. Even the most "modern" isolation procedures have the potential for altering fiber structure. Treatment of the chromosomes with endonucleases and with 0.2 mM EDTA could, for instance, cause damage by releasing any supercoil tension present in the supercoil domains of tertiary chromosome structure, by separating the fibers from the nuclear matrix, by introducing thermodynamically unstable "end effects," or by irreversibly altering the position or conformation of H1 or some other histone. Even the most gentle procedures to isolate "intact" nuclei must use rather arbitrary "physiological" salt conditions. In addition to the hazards of isolation, there are the hazards of histone modification and proteolysis during the diffraction experiments themselves, which have often involved exposures of a day or longer, usually at room temperature. The difficulty in evaluating the actual effects of these potentially disruptive effects is the lack of any assay for the structural integrity of chromosome fibers.

Electron microscopy, which has the potential of directly determining the structure of fibers by thin sectioning cells and by negatively staining individual molecules, has been useless in this role because dehydration of the fibers, even after fixation, dramatically degrades the periodic order of isolated chromatin (45), metaphase chromosomes (55) and nuclei (14, 30). In fact, 30 years of microscopy has never produced periodic images of chromatin fibers.

Some investigators have recognized the need to establish criteria by which to judge the structural integrity of isolated chromatin by performing experiments upon whole cells or isolated "intact" nuclei. In some of the earliest diffraction studies of chromosomes, Wilkins and collaborators (70, 71) reported that calf thymocytes had a 3.8-nm reflection, while sea urchin sperm had a prominent 2.7-nm and weak 3.8- and 2.1-nm reflections. Subsequently, several investigations of "intact" nuclei have been published. As pointed out by Luzzati and Nicolaieff (36, 37) and Olins et al. (47, 48), reproducible shoulders at ~11.0 and 5.5 nm are found in the diffraction patterns from chicken erythrocyte nuclei, although the 11.0 was not visible in calf thymus nuclei. However, Subirana et al. (65) and Baudy and Bram (4) were unable to detect the 11.0-nm reflection and questioned the validity of the earlier reports. In addition, Notbohm and Harbers (46) were unable to detect any maxima at 11.0, 6.0, or 3.8 nm from nuclei. Thus there have been questions raised about whether the classical "higher order" reflections even exist in patterns from native chromosomes in nuclei.

In addition to these conflicting data on the reflections present in the 2.7–11.0-nm range in nuclei, there are several reports of smaller angle reflections at low salt concentrations. These data will be analyzed in the Discussion.

Here we describe the results of our x-ray diffraction studies of chromatin in living cells, isolated nuclei, and metaphase chromosomes. Our chief aim was to determine the true spacings from chromatin in vivo where no harm has been done to the chromosome structure. It was hoped that such results would provide a standard for the quality of isolated nuclei and chromatin and possibly resolve the inconsistencies and uncertainties of previous work in this field. We were also motivated by the hope that chromatin in vivo might be more highly ordered, and thus give a better diffraction pattern, especially in the case of histone-containing sperm where unmodified histones, lack of transcription, and the constraints of volume might mean that chromatin would be in its most highly ordered state.

MATERIALS AND METHODS

Chemicals and Buffer Solutions: Wash buffer (WB) consisted of 130 mM NaCl, 5 mM KCl, 2 mM $MgCl_2$, and 10 mM HEPES, pH 7.3. Modified Earle's medium consisted of Earle's basic salt solution supplemented with 0.8% bovine serum albumen (Fraction V) and 10 mM HEPES, pH 7.3. Synthetic sea water (SSW) was prepared according to directions from a powder purchased from Instant Ocean (Eastlake, OH). The pH was adjusted to 8.3 at 5°C.

Magnesium-containing lysis buffer (MLB) consisted of 60 mM KCl, 15 mM NaCl, 2 mM $MgCl_2$, 15 mM HEPES, pH 7.3, 0.1% Nonidet P-40 (NP-40) and 10 μM phenylmethylsulfonyl fluoride (PMSF). EDTA-containing lysis buffer (ELB) was the same as MLB except that $MgCl_2$ was omitted and 2 mM EDTA was added. When detergent was omitted from these buffers they are referred to as MB and EB. The diffraction patterns with and without NP-40 were identical. Sodium tetrathionate, which eliminates both proteolysis and histone dephosphorylation, has no effect on the diffraction patterns, and was used at 1 mM concentration in some of the experiments. Buffer A consisted of 15 mM Tris[hydroxymethyl]amino methane chloride (Tris-HCl) pH 7.4, 80 mM KCl, 0.5 mM spermidine, 0.15 mM spermine, and 2 mM EDTA.

Isolation buffer (IB) for HeLa chromosomes and nuclei consisted of 10 mM HEPES, pH 7.3, 10 mM NaCl and 5 mM $MgCl_2$.

Micrococcal nuclease (EC 3.1.4.7, from *Staphylococcus aureus*) and Deoxyribonuclease I (DN-EP) from bovine pancrease (EC 3.1.4.5) were obtained from Sigma Chemical Co. (St. Louis, MO).

Cell Preparation: Chicken blood was collected in 5–20-ml samples from adult Rhode Island Red hens by cardiac puncture, using 15 U/ml heparin to prevent clotting. The erythrocytes were immediately washed three times by centrifugation (600 *g* for 5 min) in 10 vol of WB, each time discarding the buffy coat.

Lymphocytes were isolated by teasing BALB/c mouse lymph glands, spleen or thymus tissue in modified Earle's medium to disperse the cells, and then washing the cells twice in this medium by centrifugation at 600 g for 5 min. Such cells were routinely found to be 80–90% viable as assayed by the trypan blue exclusion test (see below); but in some experiments viable cells were purified to 98% viability by isopycnic banding in Percoll gradients (Pharmacia Fine Chemicals, Uppsala, Sweden).

Sea urchin (*Echinus esculentus, Psammechinus miliaris, Strongłyocentrotus purpuratus,* and *Lytechinus pictus*), scallop (*Pectin opercularis*), and dog whelk (*Nucella lapillus*) sperm were collected by excising the ripe gonads and collecting the semen in SSW. The sperm were separated from gonadal tissue by filtration through cheesecloth. 1 ml of semen was suspended in 10 ml of SSW and spun at 600 g for 5 min to remove debris. Sperm were then pelleted from the supernatant by centrifugation at 2,400 *g* for 5 min, washed twice in 10 ml SSW, and finally resuspended in 1 ml SSW.

Sperm heads were prepared by suspending washed sperm in 60 ml SSW and mixing in a Sorvall omnimixer until >95% of the flagella were sheared from the bodies but <5% of the sperm had lysed. The heads were separated from the tails by centrifugation three times at 2,000 *g* for 5 min. Heads were used immediately after preparation and remained viable in SSW during the x-ray exposure.

Cell Culture and Synchronization: HeLa S3 cells were grown in suspension in RPMI-1640 medium supplemented with 5% fetal calf serum, 100 U/ml penicillin and 100 μg/ml streptomycin. Cultures were diluted daily to 2.0 × 10^5 cells/ml.

To arrest cells in metaphase, cultures at 2.5 × 10^5 cells/ml were treated with 2.5 mM thymidine (73) for 20 h, after which the cells were pelleted, washed with 0.9% NaCl solution, and resuspended in half the original volume of fresh medium. After 4 h, 0.1 μg/ml colcemid was added to block the cells in metaphase and the cells were harvested after an additional 14 h.

Assay of Cell Viability: The viability of erythrocytes and cultured mammalian cells was determined using the criterion of cell permeability using trypan blue or fluorescein diacetate (23, 59). Somatic cells were preserved intact during x-ray experiments by keeping them in modified Earle's medium at 4°C. Sperm were preserved in SSW at 4°C. Sperm motility was used as the indicator of sperm viability.

Isolation of Cell Nuclei: Nuclei were isolated from erythrocytes, lymphocytes, and sperm cells by pelleting the cells from their storage medium at 1,000–2,000 *g* for 5 min, removing all the supernatant and rapidly suspending the cells in 10 ml MLB. The nuclei were then washed three times by pelleting at 2,000 *g* for 3 min followed by resuspension in 10 ml of buffer. The resulting white pellet was resuspended in a small volume of MLB or MB and checked by phase-contrast microscopy at × 1,000 to ensure that the nuclei had not aggregated or lysed and that the chromocenters were intact.

Rat liver nuclei were isolated in buffer A as described by Hewisch and Burgoyne (24).

HeLa interphase nuclei were isolated essentially as described by Paulson and Taylor (54). Changes in the ionic conditions of nuclei were brought about by suspending about 0.2 ml of a nuclear pellet in 10 ml of the desired buffer, followed by three cycles of pelleting (2,000 *g* for 5 min) and resuspension.

Isolation of HeLa Metaphase Chromosomes: HeLa chromosomes were isolated either as aqueous chromosomes (39) or as chromosome clusters (52) from cultures which had been arrested to 90–95% in metaphase. In both methods, cells were lysed in IB plus 0.5 M sucrose, 0.5 mM $CaCl_2$, and 0.1% NP-40 and the chromosomes were finally resuspended and washed in the same solution without the sucrose.

For experiments in which chromosomes were to be studied in 10 mM HEPES, pH 7.4, 2 mM $MgCl_2$, and 0.5 mM EGTA, they were isolated as chromosome clusters as described above except that Ca^{++} was omitted from all solutions.

Fixation, Dehydration, and Embedding of Nuclei: Nuclei in MLB were fixed with 1% glutaraldehyde for 10 min at 0°C, washed in H_2O, stained in 1% UO_2 for 10 min, and then dehydrated in ethanol. Ethanol was replaced with increasing concentrations of propylene oxide, and then Araldite or Epon, with accelerator followed by polymerization at 60°C.

Electron Microscopy: Negatively stained fibers were prepared by digestion of 1 mg/ml of chicken erythrocyte nuclei in MB supplemented with 1 mM $CaCl_2$ for 30 s at 37°C using 0.014 U/ml of micrococcal nuclease. The digestion was quenched by adding 10 mM EDTA, and the fibers were released by nitrogen decompression into EB (Langmore, J. P., and J. L. Workman, manuscript in preparation). Fibers were fixed in 0.1% glutaraldehyde in EB overnight followed by adsorption into glow discharged grids and staining with1% uranyl acetate. Embedded nuclei were thin sectioned (50–100 nm thick) and stained in 1% uranyl acetate followed by 2% lead citrate. Micrographs were recorded with a JEOL JEM 100B at 80 KV. Electron micrographs, as well as all x-ray diffraction photographs, were contact-printed to make the figures.

Nuclease Treatment of Nuclei for Diffraction: As one of the controls, chicken erythrocyte nuclei at a concentration of 1 mg/ml in MB were digested with 800 U of DNase I for 50 min at 37°C in the presence of 1 mM sodium tetrathionate in order to totally inhibit proteolysis (as determined by SDS PAGE).

Preparation and Handling of X-ray Specimens: To make an x-ray specimen, a concentrated suspension was loaded in the top of a washed glass x-ray capillary (0.7- or 1.0-mm diameter; C. Supper Co., Natick, MA) and then sedimented to a pellet at 4°C in a swinging bucket centrifuge (5 min at 100 *g* for whole cells, 2,000 *g* for nuclei, chromosomes, and spermheads). The specimen typically formed a 1–5-cm pellet in the capillary, which was then sealed with wax and maintained at 0–4°C for the duration of the experiment. To reduce radiation damage, the capillaries were continuously translated during exposure.

Samples of nuclei and chromosomes were prepared before the x-ray exposure and also after the exposure (by removing the contents of a capillary) and analyzed on 15% SDS PAGE (28). The x-ray patterns shown are representative of samples that had undergone no proteolysis of the histones. When proteolysis of H1 or H5 occurred, loss of the 30–40-nm peak occurred. Larger angle reflections could survive severe histone proteolysis.

In experiments involving whole cells it was important to insure that an x-ray exposure had no harmful effects on the cells. Lymphocytes in modified Earle's medium and sperm in SSW remain >90% viable after 8 h in capillaries at 4°C. After exposing the cells to a dose and dose rate greater than those used to record a diffraction pattern, no effect of radiation upon viability could be detected.

X-ray Cameras: The success of this study depended on the use of x-ray cameras that could record low angle scattering quickly and with very little background. We therefore built two Franks double mirror cameras (22)—one able to resolve spacings of 10 nm with a specimen to film distance of 5.3 cm and the second to resolve spacings of 80 nm using 20-cm long uncoated quartz mirrors with a specimen-to-film distance of 33.3 cm (Paulson, J. R., C. Schutt, and J. P. Langmore, manuscript in preparation). The cameras were mounted on an Elliot GX-13 rotating anode x-ray generator with a 0.1 × 1 mm focus. Later, an Elliot GX-20 with 0.1 × 2 mm focus was used with a 96-cm camera of similar design, coupled to a position sensitive detector (Technology for Energy Corporation, Knoxville, TN). Typical beam currents were 10^8 photons/s.

Analysis of Diffraction Patterns: Throughout this paper, reciprocal distances will be expressed in terms of $s = 2 \sin(\theta/2)/\lambda$, where λ is the photon wavelength (0.154 nm) and θ is the scattering angle. An arbitrary periodicity in nanometers of D in the specimen will give rise to a peak in the x-ray scattering at a reciprocal distance (1/D) nm^{-1}. Thus, when we refer to a "40-nm peak," we mean a peak in the scattering at $s = 0.025$ nm^{-1}.

Two-dimensional densitometry of the x-ray films was carried out using a Photoscan P-1000 rotating drum densitometer controlled by an interactive computer program. Specular optical densities in the range 0–2 were measured and related to x-ray intensities using data applicable to Ilford G film (43). These intensities were always corrected for the measured values of film fog and solvent scattering. The intensities near the center of the pattern could be displayed on a storage display unit to allow the operator to check the centering of the pattern to exclude the shadow of the beam stop from the analysis. Data were averaged within concentric annuli of different radii about the experimental center to give the average intensity, I, as a function of s. Because the focus and first order resolution of the camera were best in the horizontal direction, only data from the horizontal sectors are presented.

Presentation of the Data: Most of the data in this paper are presented as plots of $\log(s^2I)$ vs. s. Multiplying the intensity, I, by s^2 corrects for the random orientation of the chromatin fibers with respect to the x-ray beam, so that s^2I gives the true relative strengths (power) of the structural periodicities in the specimen by the following argument. The random orientation of the specimen causes the efficiency of recording a given diffraction peak to decrease proportionately to the square of the distance of the peak from the center of the pattern. To restore the recorded intensities to their true relative weights, we correct for this decrease in efficiency by multiplying the recorded average intensities by the Lorentz factor of s^2.

It should be noted that in the analysis of films exclusion of the beam stop is essential, since failure to do so would give rise to an artifactual peak in both the I and s^2I plots at very low angles. Similarly, correction of the optical density data for partial saturation of the film (43) is of utmost importance since otherwise an artifactual peak in s^2 at very low angles might be observed for strongly exposed films. As a result of the careful interpretation of film densities, the shape of the $\log(s^2I)$ plot is the same regardless of the exposu.e time. Moreover, our film results were compared and found to agree well with the results using the electronic position sensitive detector which of course is not subject to the potential artifacts associated with densitometry.

To avoid overlapping lines in the logarithmic plots, the intensities were multiplied by arbitrary constants. This only affects the vertical positions of the lines and does not affect the shapes whatsoever.

RESULTS

Observation of a 40-nm Reflection from Whole Chicken Erythrocytes

To investigate the structural periodicities of chromosomes in vivo, we recorded diffraction patterns from living cells. Chicken erythrocytes were chosen for study because they are quiescent, nucleated cells with few cytoplasmic organelles. Their chromosomes are transcriptionally inactive and are almost completely condensed into structures called chromocenters or chromatin bodies (13, 19). Rabbit erythrocytes, which do not have nuclei, were also chosen for study in order to control for possible contributions from non-nuclear structures.

Fig. 1 shows low angle x-ray diffraction patterns from chicken and rabbit erythrocytes. A shoulder in the intensity at ~40 nm is apparent in the chicken erythrocyte pattern but not in the rabbit erythrocyte pattern. At higher angles another shoulder is seen at ~6.0 nm in patterns from both nucleated and non-nucleated erythrocytes. This high angle shoulder is due to the intermolecular spacings of the highly concentrated intracellular hemoglobin.

The measured intensities are plotted in Fig. 2. The rabbit intensities were normalized to the chicken intensities as described earlier (30). The rabbit intensities were then subtracted from the chicken intensities to give the difference curve shown in Fig. 2*c*. This curve shows a strong maximum at ~40 nm (the mode is at 38 nm, the mean is at 41 nm) which represents the structural differences (presumably of nuclear origin) between the two cells. Higher angle difference patterns are difficult to obtain since the hemoglobin reflections dominate the diffraction patterns.

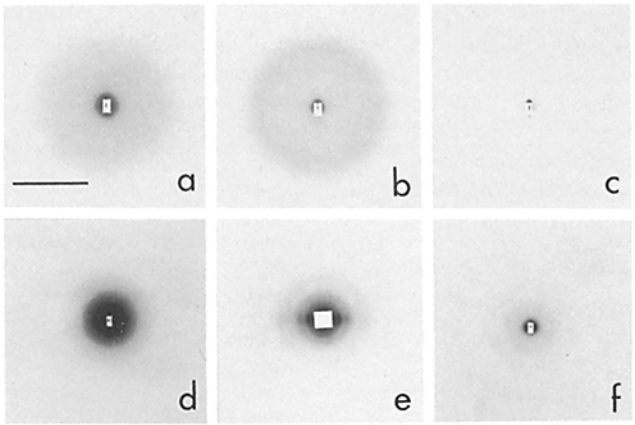

FIGURE 1 Low angle x-ray diffraction patterns of living cells, for comparison with previously published diffraction patterns of isolated chromatin. (*a*) Living chicken erythrocytes (4.2-h exposure). (*b*) Living rabbit erythrocytes (4.5-h exposure). (*c*) Solvent blank, WB in capillary (16.5-h exposure) recorded immediately after the erythrocyte exposure above, showing the extremely low camera background. (*d*) Living mouse lymph node lymphocytes in modified Earle's medium (22.5-h exposure). (*e*) Living whole sea urchin sperm *Echinus esculentus* in semen (2.5-h exposure). (*f*) Living sea urchin sperm heads in SSW (1-h exposure). Specimen-to-film distances were 33.3 cm in (*a–c*) and 21.5 cm in (*d–f*). Bars: (*a–c*) a reciprocal distance of 1/5.0 nm, and (*d–f*) 1/3.2 nm.

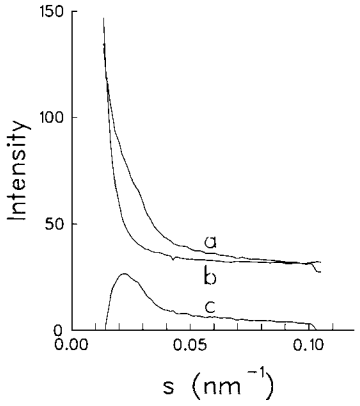

FIGURE 2 Quantitative analysis of x-ray patterns from living erythrocytes. (*a*) Measured intensities from chicken erythrocytes. (*b*) Measured intensities from rabbit erythrocytes. (*c*) Difference between chicken and rabbit erythrocyte intensities.

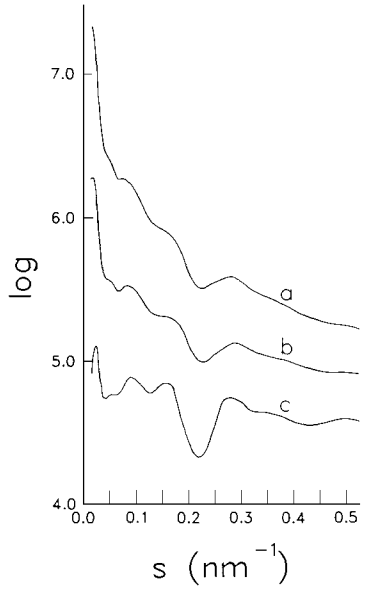

FIGURE 3 X-ray diffraction patterns of chicken erythrocytes presented as $\log(I)$, $\log(sI)$ and $\log(s^2I)$, for purposes of comparison of our data with those plotted in different forms in other studies. Vertical positions of lines are arbitrary.

Evidence That the 40-nm Reflection from Chicken Erythrocytes Is Due to Chromatin

The nuclear origin of the 40-nm peak is also demonstrated by diffraction of chicken erythrocyte nuclei isolated in MLB. Fig. 3*b* shows that the 40-nm reflection appears as a prominent peak in the plot of integrated intensity (s^2I) but it is also apparent in the plots of I and sI which are more commonly used ways of presenting such data.

Diffraction maxima are also found at 11.0, 6.0, 3.8, 2.7, and 2.1 nm, which form the well known chromatin diffraction pattern. In addition a diffraction peak is present at 18 nm. Presumably, these peaks were not seen from intact chicken erythrocytes because they were overwhelmed by the strong scattering from hemoglobin.

If the diffraction maxima from isolated nuclei are of chromosomal origin, DNase I digestion of nuclei should cause noticeable changes in the diffraction patterns. Fig. 4*a* shows the integrated diffraction intensities for intact chicken erythrocyte nuclei that had undergone a 50-min incubation at 37°C in MB. Fig. 4*b* shows the pattern for nuclei prepared at the same time but subjected to extensive digestion (50% solubility of nucleotides) with DNase I. The digested nuclei fail to show any of the reflections at 40, 18, 11.0, 6.0, and 3.8 nm. No evidence of proteolysis was detected by PAGE of a sample of the digested nuclei taken after the x-ray exposure (data not shown). Thus, all of the observed reflections from nuclei arise

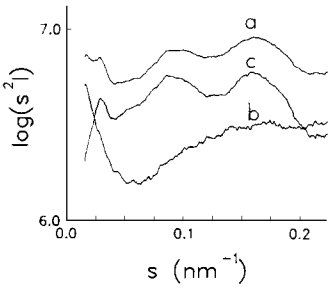

FIGURE 4 Nuclease digestion destroys the 40-nm reflection and other characteristic chromatin reflections from isolated chicken erythrocyte nuclei. (*a*) Intact chicken erythrocyte nuclei in buffer MB. (*b*) Same as *a*, but digested with DNase I. (*c*) The intensities in *b* subtracted from those in *a*. All intensities on the same absolute scale.

from chromatin structure and not from cytoplasmic contaminants, nuclear matrix, or nuclear envelope.

Additional verification of the chromosomal origin of the diffraction patterns comes from the fact that electron microscopy of isolated nuclei shows the condensed chromatin fibers to be the dominant structure present after isolation.

Chromatin X-ray Patterns from Living Mouse Lymphocyte Cells and from Isolated Lymphocyte Nuclei

Chicken erythrocytes were very useful cells for studying the 40-nm chromatin x-ray reflection in vivo, because we were able to subtract the contribution from the cytoplasm. Another approach to studying chromatin structure in vivo is to study cells that have very little cytoplasm, such as lymphocytes.

A diffraction pattern from living mouse lymphocytes in modified Earle's medium is shown in Fig. 1 *d*. The diffraction shoulders at 11.0 and 6.0 are visible. The integrated intensities from the living mouse lymphocyte cells are shown in Fig. 5 *a*. The pattern shows maxima at 33, 11.0, 6.0, 3.8, and 2.1 nm. The 2.7-nm peak is very weak, hidden by background scattering, or else not present. The same patterns were recorded from lymphocytes isolated from thymus or lymph nodes, and after purification on Percoll gradients. Similar spectra were recorded from living mouse myeloma and human lymphoblastic leukemia cells (data not shown).

To determine whether the diffraction peaks in Fig. 5 *a* were from nuclear or cytoplasmic structures, nuclei were isolated from these lymphocytes by the same method used for chicken erythrocyte nuclei. The diffraction pattern from these isolated lymphocyte nuclei is shown in Fig. 5 *b*. The lymphocyte nuclei give nearly the same pattern as the chicken erythrocyte nuclei, showing the same series of peaks at 11, 6.0, 3.8, 2.7, and 2.1 nm. In the very low angle region, however, the lymphocyte nuclei show a 33-nm reflection whereas the chicken erythrocyte nuclei show a 40-nm reflection. The 18-nm reflection, which is weak in the case of chicken erythrocyte nuclei, is not detectable from these lymphocyte nuclei.

Most importantly, the pattern of diffraction from living lymphocytes is nearly the same as that from isolated nuclei (compare Fig. 5 *a* and *b*). There are only two small differences. First, the 2.7-nm reflection is very weak in the case of whole cells. Second, the 33-nm reflection is somewhat weaker relative to the 11.0-nm reflection in the case of the isolated nuclei.

Chromatin X-ray Patterns from Living Sea Urchin and Scallop Sperm and from Isolated Sperm Nuclei

Histone-containing spermatozoa provide another example in which the entire chromatin x-ray diffraction pattern can be

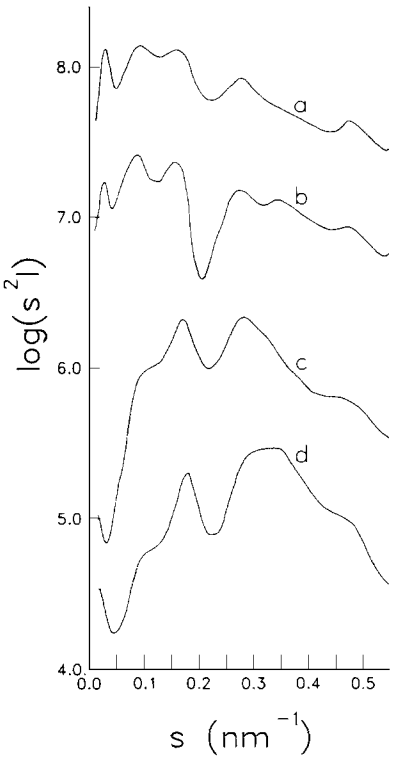

FIGURE 5 Diffraction patterns from living cells compared to isolated nuclei. Lymphocytes in this example were isolated from lymph nodes, but similar results were also obtained with lymphocytes isolated from spleen and thymus. Sperm patterns are very similar to patterns recorded from all other chromatin containing sperm. (*a*) Living mouse lymphocytes in modified Earle's medium. (*b*) Mouse lymphocyte nuclei, in buffer MB. (*c*) Living *E. esculentus* sperm heads in SSW. (*d*) *E. esculentus* sperm nuclei, in buffer MB.

observed in vivo. However, the flagella (tails) of the sperm have a strong diffraction pattern with a basic spacing of 96 nm and very strong rings at 28 and 16 nm, resulting from the structural periodicities in the axoneme. The diffraction pattern from whole sperm in semen consists of this tail pattern superimposed on the pattern from the heads (Fig. 1 *e*).

To see only the diffraction from the chromatin-containing heads we sheared the flagella from the heads. The diffraction patterns from isolated sea urchin (*E. esculentus*) sperm heads are shown in Figs. 1 *f* and 5 *c*. These heads are still living, because many still have a short motile tail and the heads have retained the same size and shape they had as intact sperm. However, since the 28- and 16-nm peaks are not detectable, remaining tails or fragments of tails are not contributing significantly to the diffraction pattern. In addition, SDS PAGE showed little tubulin in the head preparation. All five histones were present, however.

Diffraction patterns from *E. esculentus* nuclei isolated in MLB are shown in Fig. 5 *d*. The nuclei give almost the same pattern as the intact heads. Very similar results were also obtained from sperm heads and nuclei from the sea urchins *P. miliaris*, *S. purpuratus*, and *L. pictus* and from the frog *R. temporariens* and from the scallop *P. opercularis* (results not shown).

As a control, we have also studied protamine-containing sperm from *Nucella lapillus* by our techniques. Diffraction from whole sperm, sperm heads and isolated nuclei of *N. lapillus* showed a strong peak at ~2.5 nm and none of the chromatin reflections (data not shown). SDS PAGE confirmed the absence of histones.

Sperm chromatin, both in vivo and in isolated nuclei, shows diffraction peaks at 11.0, 6.0, 3.8, and 2.1 nm. The 2.7-nm peak is always very weak in diffraction patterns from heads and weak in patterns from nuclei. Spermatozoa differ from somatic cells in that the 11.0-nm is much weaker than the 6.0-nm reflection.

Sperm nuclei diffraction patterns also differ substantially

from those of lymphocyte and chicken erythrocyte nuclei in that the peak at 30–40 nm is totally absent despite an extensive search for the reflection in a variety of sperm nuclei under a variety of ionic conditions. This consistent difference between sperm and somatic cells will be discussed later.

X-ray Diffraction Patterns from Nuclei of Other Cell Types and from Mitotic Chromosomes

We would like to extend these results to the investigation of other types of living cells, but unfortunately this has not been possible for various reasons. In most cells, the volume of cytoplasm is too large, and therefore the concentration of chromatin in the cell as a whole is too low to observe a chromosome diffraction pattern above the background from cytoplasmic structures. In other cells, reflections are observed but we cannot be certain that they come from chromatin. In general, reflections from whole cells can only be reliably attributed to chromatin if we can show that the contributions from cytoplasmic structures is insignificant (as in the case of sperm and lymphocytes) or if we are able to subtract the background due to the cytoplasm (as in the case of chicken erythrocytes).

We have, however, recorded x-ray diffraction patterns from nuclei and chromosomes isolated from several different types of cells. Fig. 6 shows patterns from cultured human (HeLa) cell nuclei isolated HeLa metaphase chromosomes isolated in buffer IB plus 0.5 mM $CaCl_2$, chicken erythrocyte nuclei isolated in buffer MB, rat liver nuclei in buffer MB and in buffer A, sea urchin sperm nuclei and mouse lymphocyte nuclei. Most nuclei show peaks in the 30–40-nm region (see Table I). Rat liver nuclei do not show any diffraction peak in this region but resemble the sea urchin sperm nuclei. HeLa metaphase chromosomes have a convincing maximum at 32 nm, whereas HeLa interphase nuclei under the same conditions show, less consistently, a peak at 38 nm. Metaphase chromosomes and interphase nuclei are compared in more detail in the accompanying paper (53).

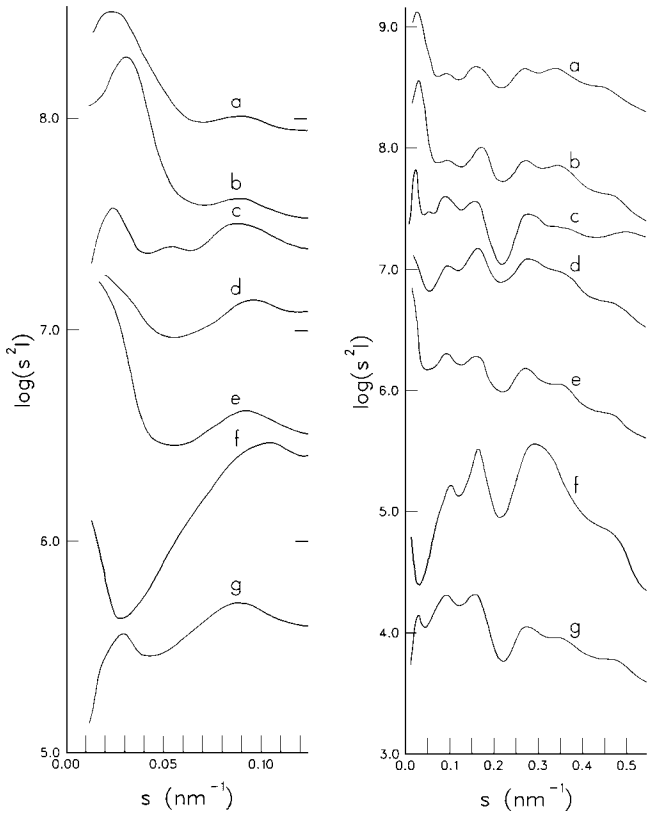

FIGURE 6 X-ray diffraction of isolated nuclei and chromosomes from several different species. (*a*) HeLa interphase nuclei in IB + 0.5 mM $CaCl_2$ + 0.1% NP-40. (*b*) HeLa metaphase chromosomes, same conditions. (*c*) Chicken erythrocyte nuclei in buffer MB. (*d*) Rat liver nuclei in buffer MB. (*e*) Rat liver nuclei in buffer A. (*f*) Sea urchin sperm (*E. esculentus*) nuclei in buffer MB. (*g*) Mouse lymphocyte nuclei in buffer MB.

The 18-nm reflection is observed only in chicken erythrocyte nuclei. Subsequent studies have confirmed that a strong reflection at ~18 nm is characteristic of chromatin in all nucleated erythrocytes (Langmore, J. P., and J. L. Workman, manuscript in preparation).

The 11-, 6.0-, 3.8-, 2.7-, and 2.1-nm reflections are quite similar in all of these cells, and Table I shows that the positions of these maxima do not vary significantly.

Evidence That the 30–40-nm X-ray Reflection Comes from Side-to-side Packing of Chromatin Fibers in Nuclei and Chromosomes

What structural feature gives rise to the 30–40-nm reflection? One possible explanation is suggested by the elegant electron microscopy of Davies and his collaborators (18, 19, 69). They reported an apparent 28–30-nm spacing between chromatin fibers in thin sections of embedded chicken erythrocytes. We embedded chicken erythrocytes and their isolated nuclei in epoxy by a similar method and obtained similar results (Fig. 7*a*). The chromocenters have a granular internal structure, apparently composed of packed thick chromatin fibers of ~30 nm diameter.

To test whether there is any relationship between the 40-nm x-ray spacing seen in chicken erythrocytes in vivo and in isolated chicken erythrocyte nuclei and the 30-nm periodicity seen in the electron microscope, we recorded x-ray diffraction patterns during the different preparative steps for microscopy (Fig. 8). Dehydration and embedding in epoxy caused a broadening and progressive shrinkage of the x-ray spacing to 31 nm, which is very close to the observed center-to-center spacing measured by Davies et al. (19) and by us. Thus the side-by-side partially ordered packing of 30-nm fibers observed by Davies in thin sections is directly correlated with more orderly packing of 30–40-nm fibers in vivo. Dehydration distorts the internal structure of the fibers as shown by loss of the 18-, 11.0-, and 6.0-nm peaks and appearance of a broad 7-nm maximum. Dehydration also produces a drastic shrinkage of the nuclei as observed by phase-contrast microscopy that is quantitatively related to the x-ray results (data not shown).

As a further test that the 40-nm reflection from chicken erythrocytes comes from side-to-side packing of chromatin fibers in chromocenters, we studied the effect of Mg^{++} concentration on the x-ray diffraction pattern. Chromocenters can be decondensed by replacing the 2 mM $MgCl_2$ in buffer MB with 2 mM EDTA to make buffer EB. Dispersal of chromocenters in this way is reversible and can be observed in the phase-contrast microscope and in the electron microscope. Nuclei in EB still possess thick chromatin fibers, but the chromocenters have disappeared, and in thin sections one sees only a homogeneous distribution of thick fibers (Fig. 7*b*). The thick fibers we observe running in the plane of the sections (arrows in Fig. 7*c*) are 25–30 nm in diameter, the same as the diameter of condensed fibers present in nuclei fixed in MB. We do not observe globular substructure in longitudinal fiber sections, nor

TABLE I

Measured Positions of Diffraction Maxima from Various Cells, Nuclei, and Chromosomes

	Very low angle	11.0 nm	6.0 nm	3.7 nm	2.7 nm	2.1 nm
Chicken erythrocytes	40.0	—	—	—	—	—
Chicken erythrocyte nuclei, buffer MB	41.0, 18.3	11.3	6.3	3.6	2.7	2.0
Mouse lymphocytes	32.6	10.7	6.1	3.6	2.6	2.1
Mouse lymphocyte nuclei, buffer MB	34.2	11.2	6.3	3.6	2.9	2.1
Sea urchin sperm heads	—	10.9	5.9	3.5	—	2.1
Sea urchin sperm nuclei buffer A	—	10.3	5.6	3.4	2.8	2.1
Sea urchin sperm nuclei, buffer MB	—	10.4	6.1	3.4	—	2.1
Scallop sperm heads	—	11.0	6.0	3.7	—	2.1
Rat liver nuclei, buffer A	—	10.3	6.0	3.6	2.7	2.0
Rat liver nuclei, buffer MB	—	10.7	6.2	3.7	2.7	2.1
HeLa nuclei, IB + 0.5 mM $CaCl_2$	38.0	11.0	6.1	3.7	2.9	2.2
HeLa metaphase chromosomes, IB + 0.5 mM $CaCl_2$	31.7	11.1	6.0	3.6	2.8	2.1

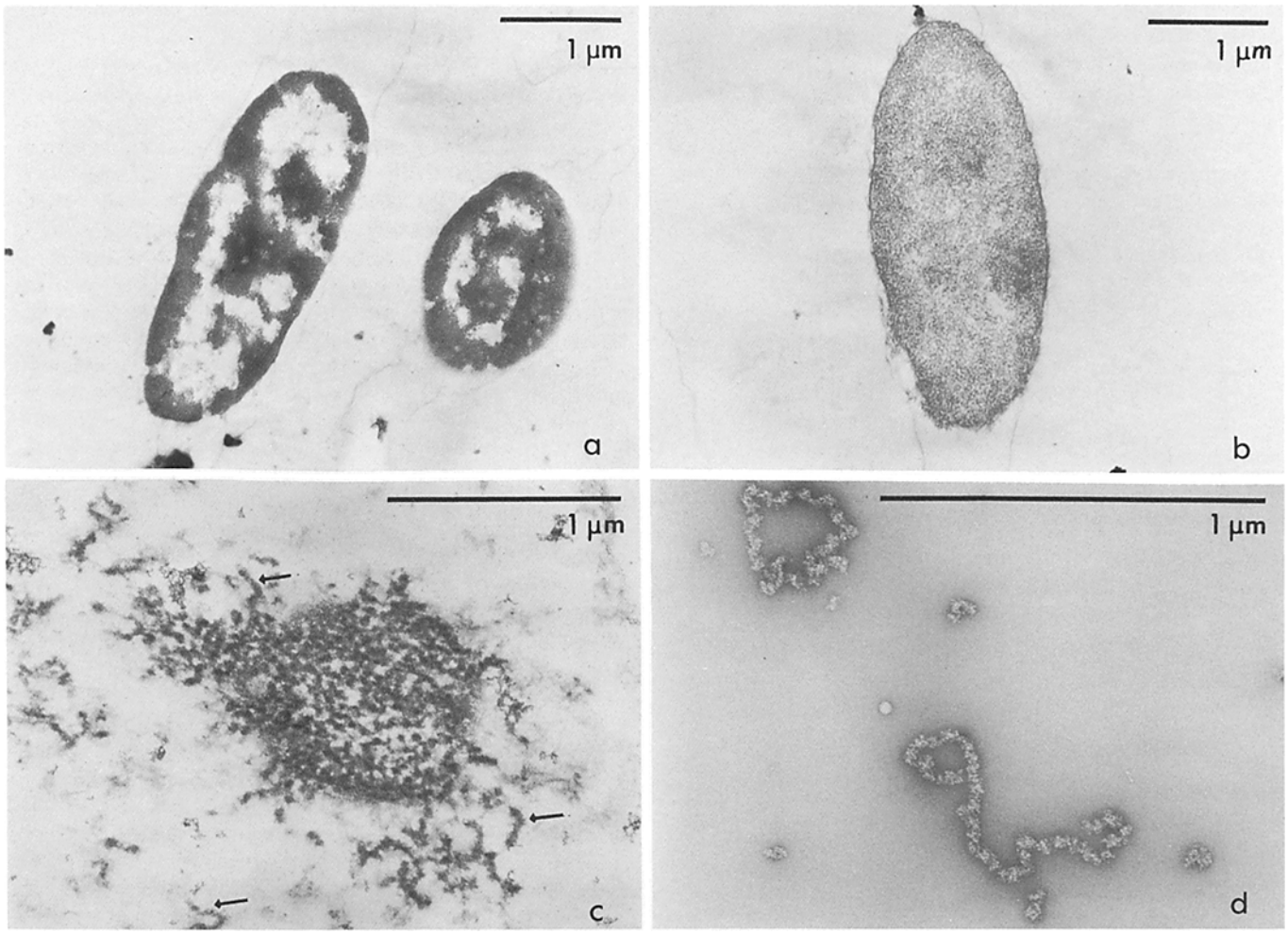

FIGURE 7 Electron micrographs of thin sections of chicken erythrocyte nuclei and fibers. (*a*) Nuclei in buffer MB, which contains 2 mM $MgCl_2$. (*b*) Nuclei in buffer EB, which is identical to MB except that $MgCl_2$ is replaced by 2 mM EDTA. In MB the thick chromatin fibers are tightly packed in the chromocenters, whereas in EB the chromocenters are dispersed. (*c*) Tangential section of the edge of a nucleus in buffer EB, with chromatin fibers spilling out into cytoplasmic space. Arrows indicate fibers within the plane of the section, confirming that the fibers appear continuous. (*d*) Negatively stained isolated fibers in EB, illustrating the relatively continuous structure.

in negatively stained fibers released from erythrocyte nuclei into EB after mild micrococcal nuclease digestion (Figs. 7 *c* and *d*).

X-ray diffraction patterns of chicken erythrocyte nuclei in buffers MB and EB are shown in Fig. 9 *a* and *b*, respectively. When Mg^{++} is removed, the 40-nm band disappears—or shifts to a longer spacing of 55 nm—presumably because the fibers become farther apart. However, the other peaks do not change their positions (Table II) even although their relative intensities change. This substantiates our hypothesis that the 40-nm spacing comes from the packing of chromatin fibers while demonstrating that the 18-, 11.0-, 6.0-, 3.8-, 2.7-, and 2.1-nm periodicities arise from internal structure of the fibers.

We made similar observations on HeLa metaphase chro-

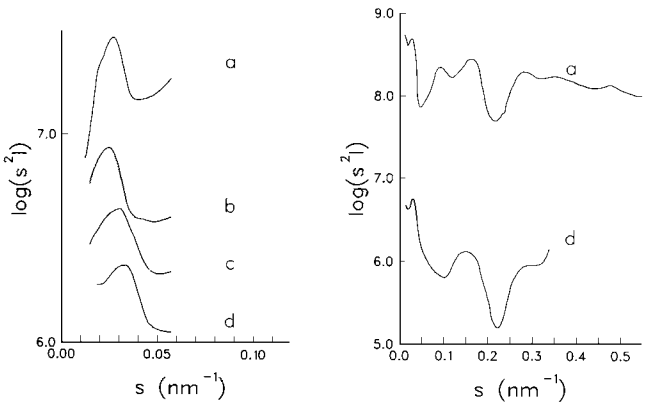

FIGURE 8 Correlation of the 40-nm reflection in chicken erythrocyte nuclei with packed 300-nm fibers seen in fixed and embedded chicken erythrocyte nuclei in the electron microscope. (*a*) Nuclei in buffer MB, unfixed. (*b*) Nuclei fixed with glutaraldehyde, stained with 1% uranyl acetate, and washed in H_2O. (*c*) Nuclei fixed, stained, and dehydrated in ethanol. (*d*) Nuclei fixed, stained, dehydrated, and embedded in Araldite.

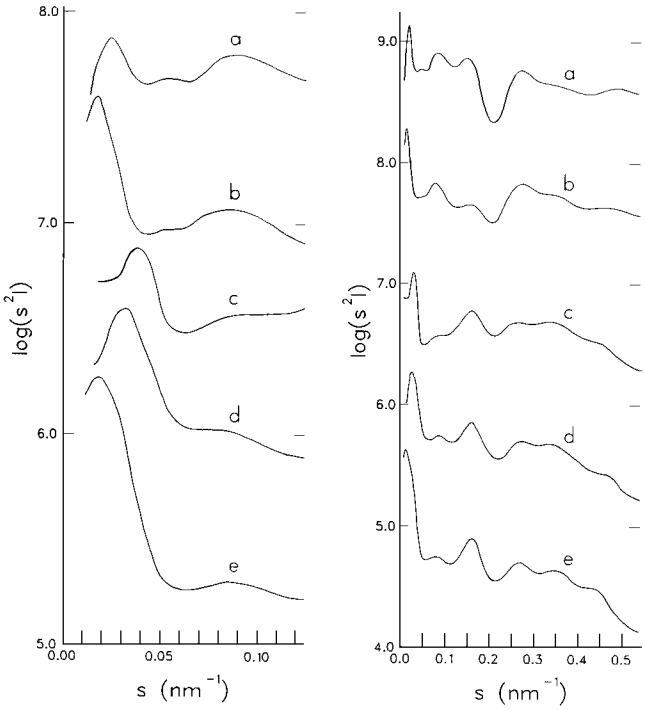

FIGURE 9 Decondensation of chromocenters or metaphase chromosomes shifts the 30-40-nm reflection to larger spacings (i.e., smaller s) but the higher angle reflections are not affected. *Left* panel shows only small angles. (a) Chicken erythrocyte nuclei in buffer MB (41-nm peak). (b) Chicken erythrocyte nuclei in buffer EB (58-nm peak). (c) HeLa metaphase chromosomes in 10 mM HEPES pH 7.4, 10 mM NaCl, 20 mM $MgCl_2$ and 2 mM $CaCl_2$ (26-nm peak). (d) HeLa metaphase chromosomes in 10 mM HEPES, pH 7.4, 10 mM NaCl, 5 mM $MgCl_2$ and 0.5 mM $CaCl_2$ (31-nm peak). (e) HeLa metaphase chromosomes in 10 mM HEPES, pH 7.4, and 2 mM $MgCl_2$ (48-nm peak).

mosomes. Mammalian metaphase chromosomes consist of tightly packed fibers. X-ray diffraction patterns were recorded from chromosomes in 20 mM Mg^{++}, 2 mM Ca^{++} (Fig. 9*c*); 5 mM Mg^{++}, 0.5 mM Ca^{++} (Fig. 9*d*); and 2 mM Mg^{++}, 0.5 mM EGTA (Fig. 9*e*). The higher angle parts of the patterns do not change markedly (see Table II) but the low angle peak shifts from 28–30 nm to 40 nm as the divalent cation concentration is decreased. This fits with our hypothesis and with the electron microscope results of Marsden and Laemmli (39) and Adolph (1) who made thin sections of chromosomes fixed under the same ionic conditions we have used.

DISCUSSION

In this work we have answered three questions: Which x-ray spacings are characteristic of chromatin in vivo? What conditions serve to preserve these spacings in isolated nuclei and metaphase chromosomes? What are the origins of these reflections? We discuss these interrelated points below.

X-RAY REFLECTIONS AT 30–40, 11.0, 6.0, 3.8, 2.7, AND 2.1 nm ARE CHARACTERISTIC OF CHROMATIN IN VIVO: Our results with mouse lymphocytes and sea urchin spermheads show clearly that reflections at 11, 6, 3.8, 2.7, and 2.1 nm are characteristic features of the x-ray diffraction pattern of chromatin in vivo. In addition, erythrocytes, and lymphocytes exhibit a 30–40-nm reflection, as yet undetected in sperm.

The interpretation of the diffraction patterns from living cells is often difficult due to the unwanted scattering from nonchromosomal origins. In some cases, for instance HeLa cells and rabbit reticulocytes (not shown), a 30-nm reflection is observed that is clearly not from chromatin but probably from the arrangement of ribosomes on the rough endoplasmic reticulum or some other cytoplasmic feature. To establish that a 30–40-nm reflection from living cells indeed comes from chromatin, it is necessary to subtract the contribution from the cytoplasm (as we have done with chicken erythrocytes) or to show that the cytoplasm does not contribute significantly (as we have done with lymphocytes and sperm by comparing the patterns from whole cells and isolated nuclei).

The fact that all the cells (and nuclei) that we examined exhibit common diffraction peaks at 11, 6, 3.8, 2.7, and 2.1 nm leads us to believe that the basic pattern of nucleosome packing is highly conserved in eucaryotic cells. Variations in the 30–40-nm reflection and its absence in spermatozoa are explained by differences in the higher orders of structure in these cells. These differences are best discussed with reference to nuclei, where more comparative data have been collected.

THE IN VIVO X-RAY DIFFRACTION PATTERN FROM CHROMATIN CAN BE PRESERVED IN ISOLATED NUCLEI AND CHROMOSOMES: We have shown that the reflections at 30–40, 11, 6, 3.8, 2.7, and 2.1 nm, which are characteristic of chromatin in vivo, are also seen in diffraction patterns from isolated nuclei, provided the right conditions are used and care is taken to prevent mechanical damage and proteolytic degradation. We found that buffer MB is particularly suitable for preserving the native chromatin fiber packing; higher or lower amounts of divalent cations promote over-compaction or under-compaction of the fibers (Langmore, J. P., and J. L. Workman, manuscript in preparation).

The biggest difference between the patterns of living cells and those of isolated nuclei is that the 2.7-nm reflection is not so strong in whole cells as in isolated nuclei. We do not yet understand the reason for this. Possibly, diffraction from the organelles reduces the contrast between the 2.7-nm reflection and its neighbors. Alternatively, a slight difference in nucleosome packing is possible.

Since other nuclei and metaphase chromosomes (from cells in which the chromatin pattern cannot be observed in vivo) give patterns similar to those of lymphocyte nuclei in the same or similar buffers, we assume that these structures have been

TABLE II

Positions of Diffraction Maxima for Chicken Erythrocyte Nuclei and HeLa Metaphase Chromosomes as a Function of a Divalent Cation Concentrations

Specimen	Reflections						
	30–40 nm	18.5 nm	11.0 nm	6.0 nm	3.7 nm	2.7 nm	2.1 nm
Chicken erythrocyte nuclei*							
(*a*) 2 mM $MgCl_2$	41.2	18.3	11.3	6.3	3.6	2.7	2.0
(*b*) 2 mM EDTA	57.6	18.9	11.6	6.0	3.6	2.8	2.1
HeLa metaphase chromosomes‡							
(*a*) 20 mM $MgCl_2$, 2 mM $CaCl_2$	26.4		11.4	5.9	3.7	2.8	2.1
(*b*) 5 mM $MgCl_2$, 0.5 mM $CaCl_2$	31.4		10.8	6.0	3.6	2.8	2.1
(*c*) 2 mM $MgCl_2$, 0.5 mM EGTA	48.3		11.4	6.0	3.6	2.7	2.2

* Chicken erythrocyte nuclei isolated in buffer MLB and then either (*a*) exposed to x-rays in MLB or (*b*) transferred to buffer EB. See Materials and Methods.

‡ HeLa chromosome clusters isolated in IB + 0.1% NP-40, then transferred to (*a*) 10 mM HEPES, pH 7.4, 10 mM NaCl, 20 mM $MgCl_2$, 2 mM $CaCl_2$; (*b*) IB + 0.5 mM $CaCl_2$; or (*c*) 10 mM HEPES, pH 7.4, 2 mM $MgCl_2$.

isolated intact. Presumably, there are slight structural differences between chromatins of different species, since the relative intensities of the various peaks in the diffraction patterns are different for different cell types, even when the same ionic conditions are used. Metaphase chromosomes and interphase nuclei of HeLa cells have a very similar structure, when compared under identical ionic conditions. More detailed comparisons are presented in the accompanying paper (53).

One of our motivations for this study was to see whether chromatin is more ordered in vivo, particularly in histone-containing sperm, since the chromatin is uniformly condensed, transcriptionally inactive and contains few nonhistone proteins or modified histones. To our disappointment, however, we found that chromatin fibers in vivo seem to be neither more nor less highly ordered than in isolated nuclei or chromosomes. Thus, the lack of sharpness of bands in diffraction patterns from isolated nuclei or chromatin fragments prepared under physiological conditions is not a preparation artifact but is due to an inherent lack of long range order in chromosomes.

The width of the 30–40-nm peak (~0.01 nm^{-1} in the best patterns) is probably due to heterogeneity in fiber diameter or disorder in fiber packing. This result is consistent with electron microscopy of nuclei, which shows a lack of crystalline packing.

The diffuse nature of the 18-, 11-, 6-, 3.8-, 2.7-, and 2.1-nm bands is not inconsistent with a highly regular internal fiber structure, because several factors can contribute to the breadth of these bands, including inherent diffuseness of the molecular Fourier transform as in the case of the Bessel functions that describe diffraction from helical fibers, and overlap of peaks with slightly different periodicities (which arise from different features of the fiber structure) because of the random orientation of the fibers. In fact, diffraction from chromatin fibers is no more diffuse than diffraction from many other randomly oriented helical molecules. For example, the diffraction patterns of double-stranded DNA in solution (7) are as diffuse as our patterns of nuclei. The inherent regularity of the chromosome fibers in comparison with other cellular structures, such as the axoneme of sea urchin sperm, is demonstrated by the domination of the chromatin scattering over that from other sources.

Our consistent observation of an 11-nm reflection from all chromatin-containing nuclei in "physiological" buffers resolves the long-standing question about the existence of an 11-nm periodicity in "intact" nuclei and chromosomes. Difficulties in sample preparation (e.g., proteolytic or nucleolytic degradation or improper ionic conditions) or excessive camera background were probably responsible for the failure of several other studies (4, 46, 65) to detect that reflection from nuclei.

THE 30–40-nm REFLECTION COMES FROM SIDE-TO-SIDE PACKING OF THICK CHROMATIN FIBERS: The 30–40-nm reflection is not an artifact of the film analysis procedure but is a real feature of the cells, nuclei and chromosomes. In particular, it does not result artifactually from computation of the integrated intensity s^2I, as claimed by Subirana (64). On the contrary, the 30–40-nm reflection is seen as a peak even in the plot of I vs. s for chicken erythrocytes, following subtraction of the background of scattering from the cytoplasm (represented by the scattering from enucleated rabbit erythrocytes). It also appears as a shoulder in plots of I and sI for lymphocytes, lymphocyte nuclei, and HeLa metaphase chromosomes (data not shown). Additional arguments for the validity of our film analysis procedure are given elsewhere (30, 31).

Second, the 30–40-nm reflection is due to chromatin. It is seen from chicken erythrocytes but not from rabbit erythrocytes. It is seen from isolated chicken erythrocyte nuclei and is destroyed when they are digested with nuclease. It is also seen from isolated lymphocyte and HeLa nuclei and especially strongly from isolated HeLa metaphase chromosomes which consist almost entirely of chromatin and in particular have no contaminating nuclear envelopes or nucleoli.

It is known from many electron microscope studies that the bulk of chromatin in higher eucaryotes consists of 30-nm thick fibers when the cells are fixed under physiological conditions. In particular, thin sections of chicken erythrocytes indicate that chromocenters (condensed patches of chromatin) have a granular internal structure with a periodicity of 30 nm, apparently composed of ordered arrays of chromatin fibers 30 nm apart. Fortunately, the thin sections of erythrocytes and their isolated nuclei reveal no nonchromosomal structures with this characteristic periodicity. A series of diffraction patterns during the process of dehydration and embedding demonstrated that the 40-nm reflection continuously exists throughout this process, although shrinking to a final value of 31 nm in the completely embedded state. We conclude that the fibers seen in thin sections are also present in vivo and that their true periodicity in vivo is closer to 35–40 nm than the 25–30 nm determined by microscopy. From the fact that the packing reflection is more narrow in vivo than in the embedded state, we conclude that the packing present in living cells is slightly more uniform than

observed in electron micrographs.

As a definitive test of our packing hypothesis we took advantage of the microscopical observation that the tightly aggregated fibers within chromocenters and metaphase chromosomes disaggregate when divalent ions are removed. The fact that only the 30–40-nm reflection moves to larger spacings when the fibers spread farther apart proves that this reflection (and only this reflection) is due to the side-by-side packing of the fibers. X-ray experiments over a range of magnesium concentrations confirm that the x-ray spacing varies as the square root of the local concentration of chromatin within chromocenters, proving that the x-ray spacing is a quantitative measure of the distance between fibers and that the mass per unit length of the fibers does not depend upon concentration of the divalent cations (Langmore, J. P., and J. L. Workman, manuscript in preparation).

These results demonstrate clearly that the 30–40-nm reflection comes from side-by-side packing of chromatin fibers in chromocenters and metaphase chromosomes. The dependence of the 30–40-nm reflection upon chromatin fiber concentration excludes the three alternative interpretations of this reflection, namely: (*a*) it is due to a helix with 40-nm repeat (4); (*b*) it is due to the first subsidiary maximum of 70-nm fibers (46); and (*c*) it is due to regular globular structures ("superbeads") along the length of the fibers (56).

Although our results are in good agreement with the microscopy of lymphocytes and erythrocytes, the results on sperm are more difficult to interpret. When sea urchin sperm are fixed in sea water the nuclei seem to be denser than somatic cell chromocenters, with faint globular or fibrillar substructure about 25 nm in size (35). When surface spread, sea urchin chromatin fibers seem to be uniform 25-nm fibers (60). However, when sperm are fixed in hypotonic media without added divalent cation, globular "superbead" structures ~36 nm in diameter are seen in thin sections (74). In spite of this microscopical evidence for fibers or "superbeads" in sea urchin sperm, our attempts to observe packing reflections from *E. esculentus*, *P. miliarus*, *S. purpuratus* and *L. pictis* have consistently failed to reveal reflections between 60 and 11 nm. Perhaps the conditions used for microscopy have caused nonspecific aggregation of sperm nucleoprotein into fibrous structures, similar to the divalent ion-sensitive fibers that are artifacts of electron microscope preparations of surface spread DNA and hemoglobin (61) and nucleoprotamine (55). Perhaps the fibers are really >60 nm in diameter and therefore beyond the resolution of our camera. Alternatively, the fibers might be so tightly packed that inadequate contrast exists between the fibers to produce a visible ring.

As shown in Table I, even though the basic high angle reflections are conserved in all cells and nuclei we studied, the variability in the low angle features make it difficult to generalize knowledge about higher order of structure in one cell type to all cells. In somatic cells and nuclei, the variation in the 30–40-nm reflection could be due to (*a*) differences in the proportion of chromatin in the chromocenters, (*b*) differences in the tightness of fiber packing in the chromocenters, and/or (*c*) differences in the diameter of the chromatin fibers. For example, rat liver nuclei probably lack a packing reflection because they have few chromocenters (thin sections show very little condensed chromatin) and thus resemble chicken erythrocyte nuclei in buffer EB. In HeLa nuclei, however, where an intermediate amount of condensed chromatin is present, the packing reflection may be a mixture of a 32-nm peak from chromocenters and a longer spacing from uncondensed chromatin, or it may just be that the fibers are not packed so closely together as in lymphocytes and HeLa metaphase chromosomes. Further quantitative studies would be needed to resolve this ambiguity. Alternatively, the observed 16% difference between the positions of the interphase and metaphase reflections could be the result of a basic difference in the symmetry of packing. For instance, assuming that all HeLa fibers are separated by a center-to-center distance of 38 nm, square packing would produce a reflection at 38 nm, whereas hexagonal packing would produce a reflection at 33 nm.

THE 18-, 11-, 6-, 3.8-, 2.7-, AND 2.1-nm REFLECTIONS RESULT FROM THE INTERNAL STRUCTURE OF CHROMOSOME FIBERS: When the positions and intensities of diffraction peaks are independent of concentration, the conclusion that those peaks arise from the internal structure of the particles is justified. Since removal of divalent cations has no effect upon the reflections at 18, 11, 6, 3.8, 2.7 and 2.1 nm, we conclude that they arise from the internal structure of the chromosome fibers and are independent of side-by-side fiber packing.

The 18-nm reflection has been seen only from erythrocytes. We cannot conclude that it reflects an erythrocyte-specific structure, however, since it is only expressed as a very weak shoulder that may, in nonerythrocyte nuclei, simply be too weak to detect. The 18-nm shoulder would be expected as an axial repeat of the chromosome fiber if, for instance, the basic helical repeat were 18 nm (two turns of the solenoid). If this were true the position of 18-nm shoulder should be as invariant as the position of the 11-nm peak.

Bram and colleagues have also observed a weak 18–20-nm reflection from nuclei and dilute fibers from erythrocytes and thymocytes (4, 8, 9). They conclude that the 20-nm shoulder arises from a coiled-coil composed of nucleosomes stacked into a 10-nm fibril that is helically coiled with a major pitch of 40–50 nm. Such as structure is not compatible with the concentration dependence of the 40-nm peak, as noted above. We have no explanation for their observations that sucrose was required to stabilize those reflections and that the 11-nm peak was always absent from nuclei. Other authors who failed to observe an 11-nm reflection also failed to observe an 18-nm feature from nuclei in 0.25 M sucrose or in 1 M hexylene glycol (that is claimed to "stabilize" the nuclei) (46). Although we have no data from nuclei in 0.25 M sucrose, data in the following paper (53) demonstrate that 1 M hexylene glycol is an inappropriate medium for studying chromatin structure.

We favor the hypothesis that the 18-nm shoulder is the first subsidiary maximum of the diffraction from cylinders of 35–40-nm diameter. These cylinders are, of course, the same thick chromatin fibers that give rise to the 40-nm packing reflection. Theoretical calculations of scattering from solid cylinders of diameter, *D*, predict a subsidiary maximum in the scattering at an apparent spacing of 0.6 *D* (38). Hollow fibers are expected to produce a scattering maximum close to the same position (42). Thus 35–40-nm fibers should produce a scattering feature at ~20 nm that would depend upon the average fiber diameter. A study of the 30–40-, 20-, and 11-nm reflections in a series of different cells has confirmed this hypothesis (Langmore, J. P., and J. L. Workman, manuscript in preparation).

There is general agreement about the origins of the higher angle reflections seen by others in chromatin and by us in nuclei. Finch and Klug (20) have provided the very reasonable proposal that the 11- and 6-nm maxima from fibers arise from the periodicity of nucleosome packing within the chromatin fiber. This proposal is correct, regardless of the exact internal

structure of the fiber, since in dilute solutions of chromatin these reflections are only seen under the salt conditions that promote thick fiber formation. As the ionic strength is decreased, the 11-nm reflection moves progressively to longer spacings as the nucleosomes move farther apart and the mass per unit length of reconstituted fibers in vitro decreases (63). In the context of the solenoid model of the fiber, the 11-nm reflection is the helical repeat, while the 6-nm reflection is due to packing of the nucleosomes along the nucleofilament (20).

Since the 3.8-, 2.7-, and 2.1-nm reflections are seen in dilute suspensions of mononucleosomes (17, 26, 50), it is reasonable to propose that they derive their contrast from features internal to the nucleosomes themselves, modulated by the packing of nucleosomes into the chromatin fiber. The data we have presented reveal no additional insight into the origins of these reflections, only that the reflections are also present in vivo and in nuclei.

The general conclusions about the origins of the x-ray reflections are summarized in Table III.

THE EXISTENCE OF 30–40-nm FIBERS IN VIVO VALIDATES THE STUDY OF CHROMOSOME FIBERS IN DILUTE SOLUTION: The packing dimensions we observe for fibers in vivo are in reasonable agreement with the measured diameters (30–35 nm) of reconstituted or fixed fibers in dilute solution (12, 33, 46, 63). In addition, the peak positions and relative magnitudes of the reflections found in dilute fibers (17, 63) resemble those we observe in nuclei.

However, as studies of the salt-induced compaction of chromatin fibers show, a family of chromatin structures exists in solution, with uniform widths but various degrees of longitudinal compaction (12, 63, 66, 67). Some of these partially compacted structures are expected to involve the same local interactions between nucleosomes that occur in the native thick fibers, and thus give rise to reflections such as those at 11 and 6 nm. A quantitative comparative study of the relative magnitudes and breadths of both the low and high angle reflections of fibers in nuclei and in dilute solution is needed before we could conclude that the isolated fibers possess totally "native" structure.

THE DIFFERENCES BETWEEN DIFFRACTION FROM CELLS AND FROM CONCENTRATED GELS REVEAL THE DIFFICULTIES IN INTERPRETING DIFFRACTION FROM CHROMATIN GELS: The distinct differences between our "native" diffraction patterns and those from concentrated gels are in the width and position of the reflections (e.g., compare the diffuse patterns of Fig. 1 to the patterns of reference 6 or 48). The fact that concentrated intact H1-depleted chromatin produces sharper reflections than do chromosomes in undisrupted cells and nuclei strongly suggests that the gels have been compressed to the point that artificial long range order has been produced. By this, we mean that the nucleosomes from different fibers might begin to stack next to each other in long rows or sheets, perhaps in a manner similar to that in crystals of nucleosome core particles (21). Although the diffraction patterns from concentrated gels might be useful in determining how nucleosomes can interact with other nucleosomes in partially dehydrated conditions, those patterns probably do not arise from the 30–40-nm chromatin fibers found in nature. If, as we suspect, the concentrated gels do not contain thick fibers, then analyses of diffraction patterns of such material (2, 15) can not give information about the internal structure of the chromatin fiber. There is, in fact, indirect evidence that fibers do not exist in concentrated gels, namely that we found that the gels whether prepared by ultracentrifugation or by partial dehydration of whole nuclei or isolated chromatin do not give the 30–40-nm peak characteristic of packed chromosome fibers (data not shown). Of course, direct evidence of the presence or absence of fibers in these gels would be provided by electron microscopy of thin sections of embedded gels. Unfortunately, we do not know of any attempts to examine the gels by microscopy.

TABLE III

Structural Repeats in Chromatin

Reflection	Source	Observed in
30–40 nm	Packing of thick fibers	Chicken erythrocytes (400 Å) Mouse lymphocytes (320 Å) HeLa nuclei (380 Å) HeLa mitotic chromosomes (320 Å)
18.5 nm	Structure of thick fiber; probably related to fiber diameter	Nucleated erythrocytes only
11.0 nm, 6.0 nm	Internal structure of fiber; packing of nucleosomes into thick fiber	All cells studied
3.7 nm, 2.7 nm, 2.1 nm	Internal structure of fiber: substructure of nucleosome	All cells studied

In summary, this study has determined some important parameters of chromosome fiber structure in vivo. The differences in the very low angle diffraction pattern among different cells, nuclei, and metaphase chromosomes illustrate the variety of ways in which chromosome fibers can be packed. The similarities in the higher angle diffraction from these sources of chromatin illustrate a common theme to the local packing of nucleosomes within the thick fibers. Our results provide both a standard for judging the quality of isolated nuclei, chromosomes and chromatin, and the basis for further experiments on chromosome fiber structure in vitro.

We are grateful to A. Klug for providing the facilities where much of this work was carried out, to C. Schutt for assistance with the diffraction experiments, and to both of them for many useful discussions. We also appreciate the expert computer programming by R. Staeden and F. Guiffrida and expert microscopy and photography by J. Workman, C. Oldenburg and V. Barr.

This work was supported by a NATO postdoctoral fellowship to J. R. Paulson, and by Public Health Service National Institutes of Health grant GM27937 to J. P. Langmore.

Received for publication 13 September 1982, and in revised form 6 December 1982.

REFERENCES

1. Adolph, K. W. 1980. Isolation and structural organization of human mitotic chromosomes. *Chromosoma (Berl.).* 76:23–33.
2. Azorin, F., A. B. Martinez, and J. A. Subirana. 1980. Organization of nucleosomes and spacer DNA in chromatin fibers. *Int. J. Biol. Macromol.* 2:81–90.
3. Baldwin, J. P., P. G. Boseley, E. M. Bradbury, and K. Ibel. 1975. The subunit structure of the eukaryotic chromosome. *Nature (Lond.).* 253:245–249.
4. Baudy, P., and S. Bram. 1979. Neutron scattering on nuclei. *Nucleic Acids Res.* 6:1721–1729.
5. Benyajati, C., and A. Worcel. 1976. Isolation, characterization and structure of the folded interphase genome of *Drosophila melanogaster*. *Cell.* 9:393–407.
6. Bradbury, E. M., H. V. Molgaard, R. M. Stephens, L. Bolund, and E. W. Johns. 1972. X-ray studies of nucleoproteins depleted of lysine-rich histone. *Eur. J. Biochem.* 31:474–482.
7. Bram, S., and W. W. Beeman. 1971. On the cross-section structure of deoxyribonucleic acid in solution. *J. Mol. Biol.* 55:311–324.
8. Bram, S., G. Butler-Browne, E. M. Bradbury, J. Baldwin, C. Reiss, and K. Ibel. 1974. Chromatin neutron and x-ray diffraction studies and high resolution melting of DNA-

histone complexes. *Biochimie.* 56:987–994.
9. Bram, S., G. Butler-Browne, P. Baudy, and K. Ibel. 1975. Quaternary structure of chromatin. *Proc. Natl. Acad. Sci. USA.* 72:1043–1045.
10. Brasch, K. 1976. Studies on the role of histones H1 (f1) and H5 (f2c) in chromatin structure. *Exp. Cell Res.* 101:396–410.
11. Callan, H. G., and L. Lloyd. 1960. Lampbrush chromosomes of crested newts *Triturus cristatus. Philos. Trans. R. Soc. Lond. B. Biol. Sci.* 243:135–219.
12. Campbell, A. M., R. I. Cotter, and J. F. Pardon. 1978. Light scattering measurements supporting helical structures for chromatin in solution. *Nucleic Acids Res.* 5:1571–1580.
13. Cameron, I. L., and D. M. Prescott. 1963. RNA and protein metabolism in the maturation of the nucleated chicken erythrocyte. *Exp. Cell Res.* 30:609–612.
14. Carlson, R. D., and A. L. Olins. 1974. Effects of formaldehyde and urea on low angle x-ray diffraction of chromatin. *Fed. Proc.* 33:1538.
15. Carpenter, B. G., J. P. Baldwin, E. M. Bradbury, and K. Ibel. 1976. Organization of subunits in chromatin. *Nucleic Acids Res.* 3:1739–1746.
16. Cook, P. R., and I. A. Brazell. 1975. Supercoils in human DNA. *J. Cell Sci.* 19:261–279.
17. Damaschun, H., G. Damaschun, V. A. Pospelov, and V. I. Vorobiev. 1980. X-ray small angle scattering study of mononucleosomes and of the close packing of nucleosomes in polynucleosomes. *Mol. Biol. Reports.* 6:185–191.
18. Davies, H. G. 1968. Electron-microscope observations on the organization of heterochromatin in certain cells. *J. Cell Sci.* 3:129–150.
19. Davies, H. G., A. B. Murray, and M. E. Walmsley. 1974. Electron-microscope observations on the organization of the nucleus in chicken erythrocytes and a superunit thread hypothesis for chromosome structure. *J. Cell Sci.* 16:261–299.
20. Finch, J. T., and A. Klug. 1976. Solenoidal model for superstructure in chromatin. *Proc. Natl. Acad. Sci. USA.* 73:1897–1901.
21. Finch, J. T., L. C. Lutter, D. Rhodes, R. S. Brown, B. M. Rushton, M. Levitt, and A. Klug. 1977. Structure of nucleosome core particles of chromatin. *Nature (Lond.).* 269:29–36.
22. Franks, A. 1958. Some developments and applications of microfocus x-ray diffraction techniques. *Br. J. Appl. Phys.* 9:349–352.
23. Guilbault, G. G., and D. N. Kramer. 1964. Fluorometric determination of lipase, acylase, alpha-, and gamma-chromotrypsin and inhibitors of these enzymes. *Anal. Chem.* 36:409–412.
24. Hewisch, D. R., and L. A. Burgoyne. 1973. Chromatin sub-structure. The digestion of chromatin DNA at regularly spaced sites by a nuclear deoxyribonuclease. *Biochem. Biophys. Res. Commun.* 52:504–510.
25. Hozier, J., M. Renz, and P. Nehls. 1977. The chromosome fiber: evidence for an ordered superstructure of nucleosomes. *Chromosoma (Berl.).* 62:301–317.
26. Hjelm, R. P., G. G. Kneale, P. Suau, J. P. Baldwin, E. M. Bradbury, and K. Ibel. 1977. Small angle neutron scattering studies of chromatin subunits in solution. *Cell.* 10:139–151.
27. Jorcano, J. L., G. Meyer, L. A. Day, and M. Renz. 1980. Aggregation of small oligonucleosomal chains into 300 Å globular particles. *Proc. Natl. Acad. Sci. USA.* 77:6443–6447.
28. Laemmli, U. K., and M. Favre. 1973. Maturation of the head of bacteriophage T4 I. DNA packaging events. *J. Mol. Biol.* 80:575–599.
29. Laemmli, U. K., S. M. Cheng, K. W. Adolph, J. R. Paulson, J. A. Brown, and W. R. Baumbach. 1978. Metaphase chromosome structure: the role of nonhistone proteins. *Cold Spring Harbor Symp. Quant. Biol.* 42:351–360.
30. Langmore, J. P., and C. Schutt. 1980. The higher order structure of chicken erythrocyte chromosomes *in vivo. Nature (Lond.).* 288:620–622.
31. Langmore, J. P., and C. Schutt. 1981. Low-angle x-ray scattering of chromatin. *Nature (Lond.)* 291:359–360.
32. Langmore, J. P., and J. C. Wooley. 1975. Chromatin architecture: investigation of a subunit of chromatin by dark-field electron microscopy. *Proc. Natl. Acad. Sci. USA.* 72:2691–2695.
33. Lee, K. S., M. Mandelkern, and D. M. Crothers. 1981. Solution structural studies of chromatin fibers. *Biochemistry.* 20:1438.
34. Lilley, D. M. J., and J. F. Pardon. 1979. Structure and function of chromatin. *Annu. Rev. Genet.* 13:197–233.
35. Longo, F. J., and E. Anderson. 1969. Sperm differentiation in the sea urchins *Arbacia punctulata* and *Strongylocentrotus purpuratus. J. Ultrastruct. Res.* 27:486–509.
36. Luzzati, V., and A. Nicolaieff. 1959. Etude par diffusion des rayons X aux petits angles des gels d'acide desoxyribonucleique et de nucleoproteines. *J. Mol. Biol.* 1:127–133.
37. Luzzati, V., and A. Nicolaieff. 1963. The structure of nucleohistones and nucleoprotamines. *J. Mol. Biol.* 7:142–163.
38. Malmon, A. G. 1957. Small angle x-ray scattering functions for ellipsoids of revolution and right circular cylinders. *Acta Crystallogr. Sect. B Struct. Crystallogr. Cryst. Chem.* 10:639–642.
39. Marsden, M. P. F., and U. K. Laemmli. 1979. Metaphase chromosome structure: evidence for a radial loop model. *Cell.* 17:849–858.
40. McGhee, J. D., and G. Felsenfeld. 1980. Nucleosome structure. *Annu. Rev. Biochem.* 49:1115–1156.
41. McGhee, J. D., D. C. Rau, E. Charney, and G. Felsenfeld. 1981. Orientation of the nucleosome within the higher order structure of chromatin. *Cell.* 22:87–96.
42. Mittelbach, P., and G. Porod (1961). Zur Röntgenkleinwinkelstreuung verdünnter kolloider Systeme VI. Die Berechnung der Streukurven von elliptischen Zylindern und Hohlzylindern. *Acta Physica Austriaca.* 14:405–439.
43. Morimoto, H., and R. Uyeda. 1963. A second comparison of various commercially available x-ray films. *Acta Crystallogr. Sect. B Struct. Crystallogr. Cryst. Chem.* 16:1107–1119.
44. Murray, K., E. M. Bradbury, C. Crane-Robinson, R. M. Stephens, A. J. Haydon, and A. R. Peacocke. 1970. The dissociation of chicken erythrocyte deoxyribonucleoprotein and some properties of its partial nucleoproteins. *Biochem. J.* 120:859–871.
45. Nicolaieff, A. 1967. Structure of nucleoproteins studied by means of small-angle scattering. *In* Small Angle X-ray Scattering. H. Brumberger, editor. Gordon and Breach, New York. 221–241.
46. Notbohm, H., and E. Harbers. 1981. Small angle x-ray scattering of intact and lysing cell nuclei. *Int. J. Biol. Macromol.* 3:311–314.
47. Olins, A. L., R. D. Carlson, and D. E. Olins. 1975. Visualization of chromatin substructure: bodies. *J. Cell Biol.* 64:528–537.
48. Olins, E. D., and A. L. Olins. 1972. Physical studies of isolated eucaryotic nuclei. *J. Cell Biol.* 53:715–736.
49. Pardon, J. F., B. M. Richard, and R. I. Cotter. 1973. X-ray diffraction studies on oriented nucleohistone gels. *Cold Spring Harbor Symp. Quant. Biol.* 38:75–81.
50. Pardon, J. F., D. L. Worcester, J. C. Wooley, R. I. Cotter, D. M. J. Lilley, and B. M. Richards. 1977. The structure of the chromatin core particles in solution. *Nucleic Acids Res.* 4:3199–3214.
51. Paulson, J. R. 1980. Sulfhydryl reagents prevent dephosphorylation and proteolysis of histones in isolated HeLa metaphase chromosomes. *Eur. J. Biochem.* 111:189–197.
52. Paulson, J. R. 1983. Isolation of chromosome clusters from metaphase arrested HeLa cells. *Chromosoma (Berl.).* 85:571–581.
53. Paulson, J. R., and J. P. Langmore. 1983. Low angle x-ray diffraction studies of HeLa metaphase chromosomes: the effects of histone phosphorylation and chromosome isolation procedure. 96:1132–1137.
54. Paulson, J. R., and S. S. Taylor. 1982. Phosphorylation of histones 1 and 3 and nonhistone high mobility group 14 by an endogenous kinase in HeLa metaphase chromosomes. *J. Biol. Chem.* 257:6064–6072.
55. Pooley, A. S., J. F. Pardon, and B. M. Richards. 1974. The relation between the unit thread of chromosomes and isolated nucleohistone. *J. Mol. Biol.* 85:533–549.
56. Renz, M., P. Nehls, and J. Hozier. 1977. Involvement of histone H1 in the organization of the chromosome fiber. *Proc. Natl. Acad. Sci. USA.* 74:1879–1883.
57. Richards, B. M., and J. F. Pardon. 1970. The molecular structure of nucleohistone (DNH). *Exp. Cell Res.* 62:184–196.
58. Richards, B. M., J. Pardon, D. Lilley, R. Cotter, J. Wooley, and D. Worcester. 1977. The substructure of nucleosomes. *Cell Biol. Int. Rep.* 1:107–116.
59. Seglen, P. O. 1976. Preparation of isolated rat liver cells. *In* Cell Biology. D. M. Prescott, editor. Academic Press, New York. *Vol.* 13:29–83.
60. Solari, A. J. 1965. Structure of the chromatin in sea urchin sperm. *Proc. Natl. Acad. Sci. USA.* 53:503–511.
61. Solari, A. J. 1971. Experimental changes in the width of the chromatin fibers from chicken erythrocytes. *Exp. Cell Res.* 67:161–170.
62. Sperling, L., and A. Klug. 1977. X-ray studies on "native" chromatin. *J. Mol. Biol.* 112:253–263.
63. Suau, P., E. M. Bradbury, and J. P. Baldwin. 1979. Higher order structures of chromatin in solution. *Eur. J. Biochem.* 97:593–602.
64. Subirana, J. A. 1981. Low angle x-ray scattering of chromatin. *Nature (Lond.).* 291:359.
65. Subirana, J. A., L. C. Puigjaner, J. Roca, R. Lloips, and P. Suau. 1975. X-ray diffraction of nucleohistones from spermatozoa. *In* The Structure and Function of Chromatin. Ciba Foundation Symposium. D. W. Fitzsimmons and D. E. W. Wolfstenholme, editors. Associated Scientific Publishers, Amsterdam. 28:157–174.
66. Thoma, F., and T. Koller. 1977. Influence of histone H1 on chromatin structure. *Cell.* 12:101–107.
67. Thoma, F., T. Koller, and A. Klug. 1979. Involvement of histone H1 in the organization of the nucleosome and of the salt-dependent superstructures of chromatin. *J. Cell Biol.* 83:403–427.
68. Van Holde, K. E., C. G. Sahasrabuddhe, and B. R. Shaw. 1974. A model for particulate structure in chromatin. *Nucleic Acids Res.* 1:1579–1586.
69. Walmsley, M. E., and H. G. Davies. 1975. Ultrastructural and biochemical observations on interphase nuclei isolated from chicken erythrocytes. *J. Cell. Sci.* 17:113–139.
70. Wilkins, M. H. F. 1956. Physical studies of the molecular structure of deoxyribose nucleic acid and nucleoprotein. *Cold Spring Harbor Symp. Quant. Biol.* 21:75–90.
71. Wilkins, M. H. F., G. Zubay, and H. R. Wilson. 1959. X-ray diffraction studies of the molecular structure of nucleohistone and chromosomes. *J. Mol. Biol.* 1:179–185.
72. Worcel, A., S. Strogatz, and D. Riley. 1981. Structure of chromatin and the linking number of DNA. *Proc. Natl. Acad. Sci. USA.* 78:1461–1465.
73. Xeros, N. 1962. Deoxyriboside control and synchronisation of mitosis. *Nature (Lond.).* 194:682–683.
74. Zentgraf, M., U. Müller, and W. Franke. 1980. Supranucleosomal organization of sea urchin sperm chromatin in regularly arranged 40 to 50 nm large granular subunits. *Eur. J. Cell Biol.* 20:254–264.
75. Zubay, G., and P. Doty. 1959. The isolation and properties of deoxyribonucleoprotein particles containing single nucleic acid molecules. *J. Mol. Biol.* 1:1–20.